

Supramolecular Gel Based on a Perylene Diimide Dye: Multiple Stimuli Responsiveness, Robustness, and Photofunction

Elisha Krieg,[†] Elijah Shirman,[†] Haim Weissman,[†] Eyal Shiloni,[‡] Sharon G. Wolf,[‡]
Iddo Pinkas,[§] and Boris Rybtchinski*,[†]

*Departments of Organic Chemistry, Plant Sciences, and Chemical Research Support,
Weizmann Institute of Science, Rehovot 76100, Israel*

Received May 14, 2009; E-mail: boris.rybtchinski@weizmann.ac.il

Abstract: Design of an extensive supramolecular three-dimensional network that is both robust and adaptive represents a significant challenge. The molecular system **PP2b** based on a perylene diimide chromophore (PDI) decorated with polyethylene glycol groups self-assembles in aqueous media into extended supramolecular fibers that form a robust three-dimensional network resulting in gelation. The self-assembled systems were characterized by cryo-TEM, cryo-SEM, and rheological measurements. The gel possesses exceptional robustness and multiple stimuli-responsiveness. Reversible charging of **PP2b** allows for switching between the gel state and fluid solution that is accompanied by switching on and off the material's birefringence. Temperature triggered deswelling of the gel leads to the (reversible) expulsion of a large fraction of the aqueous solvent. The dual sensibility toward chemical reduction and temperature with a distinct and interrelated response to each of these stimuli is pertinent to applications in the area of adaptive functional materials. The gel also shows strong absorption of visible light and good exciton mobility (elucidated using femtosecond transient absorption), representing an advantageous light harvesting system.

Introduction

Gels are exceptionally versatile materials.^{1–4} In particular, stimuli-responsive gels are of great importance for the development of adaptive multifunctional systems (smart materials). It has been demonstrated that some gels respond to temperature,^{11,12} redox agents^{13–16} and other chemical entities,^{17,18} electric field,¹⁹

light,^{20–24} and sound.²⁵ A response to multiple stimuli has also been demonstrated.^{26–28} Multiple stimuli-responsiveness is especially beneficial for creation of smart materials.^{29,30}

Supramolecular gels that are composed of small molecules held together by noncovalent interactions possess advantageous properties for creation of responsive materials due to the dynamic character of noncovalent bonding.⁵ Such gels are based

[†] Department of Organic Chemistry.

[‡] Department of Chemical Research Support.

[§] Department of Plant Sciences.

- (1) Sangeetha, N. M.; Maitra, U. *Chem. Soc. Rev.* **2005**, *34*, 821–836.
- (2) Hirst, A. R.; Escuder, B.; Miravet, J. F.; Smith, D. K. *Angew. Chem., Int. Ed.* **2008**, *47*, 8002–8018.
- (3) Xie, P.; Zhang, R. *J. Mater. Chem.* **2005**, *15*, 2529–2550.
- (4) Maeda, S.; Hara, Y.; Sakai, T.; Yoshida, R.; Hashimoto, S. *Adv. Mater.* **2007**, *19*, 3480–3484.
- (5) Jong, J.; Feringa, B.; Esch, J. Responsive Molecular Gels. In *Molecular Gels: Materials with Self-Assembled Fibrillar Networks*; Weiss, R. G., Terech, P., Eds.; Springer: Dordrecht, 2006; pp 895–927.
- (6) Maeda, H. *Chem.—Eur. J.* **2008**, *14*, 11274–11282.
- (7) Hendrickson, G. R.; Lyon, L. A. *Soft Matter* **2009**, *5*, 29–35.
- (8) Ahn, S. K.; Kasi, R. M.; Kim, S. C.; Sharma, N.; Zhou, Y. X. *Soft Matter* **2008**, *4*, 1151–1157.
- (9) Ishii, T.; Shinkai, S. *Top. Curr. Chem.* **2005**, *258*, 119–160.
- (10) Sidorenko, A.; Krupenkin, T.; Taylor, A.; Fratzl, P.; Aizenberg, J. *Science* **2007**, *315*, 487–490.
- (11) Yoshida, R.; Uchida, K.; Kaneko, Y.; Sakai, K.; Kikuchi, A.; Sakurai, Y.; Okano, T. *Nature* **1995**, *374*, 240–242.
- (12) Kiyonaka, S.; Sugiyasu, K.; Shinkai, S.; Hamachi, I. *J. Am. Chem. Soc.* **2002**, *124*, 10954–10955.
- (13) Kawano, S.-i.; Fujita, N.; Shinkai, S. *J. Am. Chem. Soc.* **2004**, *126*, 8592–8593.
- (14) Chen, J.; McNeil, A. J. *J. Am. Chem. Soc.* **2008**, *130*, 16496–16497.
- (15) Tomatsu, I.; Hashidzume, A.; Harada, A. *Macromol. Rapid Commun.* **2006**, *27*, 238–241.
- (16) Wang, C.; Zhang, D.; Zhu, D. *J. Am. Chem. Soc.* **2005**, *127*, 16372–16373.
- (17) Deng, W.; Yamaguchi, H.; Takashima, Y.; Harada, A. *Angew. Chem., Int. Ed.* **2007**, *46*, 5144–5147.
- (18) Kim, H.-J.; Lee, J.-H.; Lee, M. *Angew. Chem., Int. Ed.* **2005**, *44*, 5810–5814.
- (19) Mizoshita, N.; Suzuki, Y.; Kishimoto, K.; Hanabusa, K.; Kato, T. *J. Mater. Chem.* **2002**, *12*, 2197–2201.
- (20) Guerzo, A.; Pozzo, J.-L. Photoresponsive Gels. In *Molecular Gels: Materials with Self-Assembled Fibrillar Networks*; Weiss, R. G., Terech, P., Eds.; Springer: Dordrecht, 2006; pp 817–855.
- (21) Matsumoto, S.; Yamaguchi, S.; Ueno, S.; Komatsu, H.; Ikeda, M.; Ishizuka, K.; Iko, Y.; Tabata, K. V.; Aoki, H.; Ito, S.; Noji, H.; Hamachi, I. *Chem.—Eur. J.* **2008**, *14*, 3977–3986.
- (22) Peng, F.; Li, G.; Liu, X.; Wu, S.; Tong, Z. *J. Am. Chem. Soc.* **2008**, *130*, 16166–16167.
- (23) Sumaru, K.; Ohi, K.; Takagi, T.; Kanamori, T.; Shinbo, T. *Langmuir* **2006**, *22*, 4353–4356.
- (24) Akazawa, M.; Uchida, K.; de Jong, J. J. D.; Areephong, J.; Stuart, M.; Caroli, G.; Browne, W. R.; Feringa, B. L. *Org. Biomol. Chem.* **2008**, *6*, 1544–1547.
- (25) Naota, T.; Koori, H. *J. Am. Chem. Soc.* **2005**, *127*, 9324–9325.
- (26) Weng, W.; Beck, J. B.; Jamieson, A. M.; Rowan, S. J. *J. Am. Chem. Soc.* **2006**, *128*, 11663–11672.
- (27) Liu, J.; He, P.; Yan, J.; Fang, X.; Peng, J.; Liu, K.; Fang, Y. *Adv. Mater.* **2008**, *20*, 2508–2511.
- (28) Komatsu, H.; Matsumoto, S.; Tamaru, S.-i.; Kaneko, K.; Ikeda, M.; Hamachi, I. *J. Am. Chem. Soc.* **2009**, *131*, 5580–5585.
- (29) Yerushalmi, R.; Scherz, A.; van der Boom, M. E.; Kraatz, H.-B. *J. Mater. Chem.* **2005**, *15*, 4480–4487.
- (30) Yoshida, M.; Lahann, J. *ACS Nano* **2008**, *2*, 1101–1107.

on self-assembly of molecular subunits into one-dimensional fibers^{31,32} that further assemble into a three-dimensional network. As the structure of supramolecular gels is determined by a hierarchy of various structural elements, their response can take place on different structural levels.^{33–35} Importantly, most supramolecular gels are characterized by a gel to sol transition at moderate temperatures as the strength of noncovalent bonding is comparable to ambient thermal energy.⁵ Thus, although very advantageous as regards stimuli responsiveness, supramolecular gels lack robustness. In general, design of an extensive supramolecular three-dimensional network that is both robust³⁶ and adaptive represents a significant challenge.

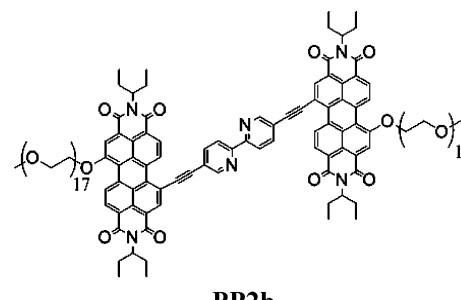
Water is an advantageous medium for self-assembly,³⁷ which is characterized by strong hydrophobic forces when extended hydrophobic surfaces are involved.^{38–40} At the same time, reversible attenuation of hydrophobicity is feasible and can lead to a high degree of adaptivity. We have recently demonstrated that reversible depolymerization of supramolecular polymers assembled in aqueous medium can be achieved through charging/discharging of the aromatic subunits.⁴¹ Hence, *supramolecular hydrogels based on extended aromatic systems* can result in both robust and responsive (through aromatic charging) networks. In addition, such gels, if based on chromophores, should have advantageous photonic and electronic characteristics. For example, supramolecular gels based on dyes have been found to possess excellent light harvesting properties.^{1,9,42} Recent examples include organogels based on π -conjugated molecular systems such as oligo(phenylenevinylene)s,^{42–44} platinum acetylides oligomers,⁴⁵ and perylene diimides.^{46–48} In contrast to these *organogels*, the area of light harvesting *hydrogels* is largely unexplored.^{49,50}

Herein we report on a supramolecular perylene diimide-based gel, which assembles due to hydrophobic interactions. It is

robust, yet adaptive (demonstrates multiple stimuli-responsiveness), and possesses advantageous light harvesting properties.

Results and Discussion

Following our interest in the self-assembly of nanoscale photofunctional systems in an aqueous medium,^{41,57} we have synthesized compound **PP2b** (synthesis and characterization are described in the Supporting Information). **PP2b** is based on a perylene diimide (PDI) chromophore that is known for its exceptional thermal and photochemical stability, strong absorption of visible light, and high fluorescence quantum yields.^{51,52} The extended π -conjugated core of **PP2b** containing PDI, bipyridyl, and ethynyl moieties is strongly hydrophobic, while hydrophilic polyethylene glycol (PEG) side chains result in overall amphiphilicity of **PP2b**. The bipyridyl (bipy) linker was chosen because of its planar structure. Thus, **PP2b** possesses an extended flat aromatic core with a strong propensity for stacking and enhanced hydrophobicity. Upon stacking of **PP2b** in an aqueous medium several new hydrophobic (or partially hydrophobic) interfaces may develop,^{41,57} leading to a hierarchical multidimensional character of assembly. Additionally, bipy is a good ligand for a variety of metals, making it possible to tune the **PP2b** structure and properties via metal coordination. This represents a subject of future studies.



PP2b

PP2b is disaggregated in various organic solvents, such as chloroform, dichloromethane, and THF, showing sharp visible light absorption bands, strong fluorescence, and sharp peaks in the NMR spectrum (see Figures S1, S2). Self-assembly of **PP2b** is induced by addition of water to a solution of the compound in THF. UV/vis spectroscopy of **PP2b** in different water/THF mixtures indicates aggregation (Figure 1). Thus, increasing water content leads to broadening of the absorption bands, accompanied by some loss of absorption intensity, a slight red shift, and an inversion of relative intensities of 0–0 and 0–1 electronic transitions, typical of face-to-face stacking of PDI molecules.⁵¹ In a disaggregating solvent such as THF, **PP2b** shows strong fluorescence ($\lambda_{\text{max}} = 603 \text{ nm}$, quantum yield = 58%) that is quenched upon addition of water (Figure S3). In solutions containing 20 vol% THF content or less, fluorescence is quenched almost quantitatively, indicating a high degree of aggregation. The very low residual fluorescence of **PP2b** in this solvent mixtures is red-shifted ($\lambda_{\text{max}} = 685 \text{ nm}$), characteristic of excimer fluorescence.⁵³ The water/THF mixtures of **PP2b** are homogeneous and stable over time as long as the THF content is above 10 vol%. Below this content the mixture

- (31) Schenning, A. P. H. J.; Meijer, E. W. *Chem. Commun.* **2005**, 3245–3258.
- (32) Zang, L.; Che, Y.; Moore, J. S. *Acc. Chem. Res.* **2008**, *41*, 1596–1608.
- (33) Estroff, L. A.; Hamilton, A. D. *Chem. Rev.* **2004**, *104*, 1201–18.
- (34) Hecht, S. *Mater. Today* **2005**, 48–55.
- (35) Elemans, J. A. A. W.; Rowan, A. E.; Nolte, R. J. M. *J. Mater. Chem.* **2003**, *13*, 2661–2670.
- (36) Diaz, D. D.; Cid, J. J.; Vazquez, P.; Torres, T. *Chem.—Eur. J.* **2008**, *14*, 9261–9273.
- (37) Oshovsky, G. V.; Reinhoudt, D. N.; Verboom, W. *Angew. Chem., Int. Ed.* **2007**, *46*, 2366–2393.
- (38) Meyer, E. A.; Castellano, R. K.; Diederich, F. *Angew. Chem., Int. Ed.* **2003**, *42*, 1210–1250.
- (39) Chandler, D. *Nature* **2005**, *437*, 640–647.
- (40) Ball, P. *Chem. Rev.* **2008**, *108*, 74–108.
- (41) Baram, J.; Shirman, E.; Ben-Shitrit, N.; Ustinov, A.; Weissman, H.; Pinkas, I.; Wolf, S. G.; Rybtchinski, B. *J. Am. Chem. Soc.* **2008**, *130*, 14966–14967.
- (42) Ajayaghosh, A.; Praveen, V. K.; Vijayakumar, C. *Chem. Soc. Rev.* **2008**, *37*, 109–22.
- (43) Ajayaghosh, A.; George, S. J.; Praveen, V. K. *Angew. Chem., Int. Ed.* **2003**, *42*, 332–335.
- (44) van Herrikhuyzen, J.; George, S. J.; Vos, M. R. J.; Sommerdijk, N. A. J. M.; Ajayaghosh, A.; Meskers, S. C. J.; Schenning, A. P. H. J. *Angew. Chem., Int. Ed.* **2007**, *46*, 1825–1828.
- (45) Cardolaccia, T.; Li, Y.; Schanze, K. S. *J. Am. Chem. Soc.* **2008**, *130*, 2535–2545.
- (46) Sugiyasu, K.; Fujita, N.; Shinkai, S. *Angew. Chem.* **2004**, *116*, 1249–1253.
- (47) Würthner, F.; Bauer, C.; Stepanenko, V.; Yagai, S. *Adv. Mater.* **2008**, *20*, 1695–1698.
- (48) Würthner, F.; Hanke, B.; Lysetska, M.; Lambright, G.; Harms, G. S. *Org. Lett.* **2005**, *7*, 967–970.
- (49) Nakashima, T.; Kimizuka, N. *Adv. Mater.* **2002**, *14*, 1113–1116.
- (50) Montalti, M.; Dolei, L. S.; Prodi, L.; Zaccheroni, N.; Stuart, M. C. A.; van Bommel, K. J. C.; Friggeri, A. *Langmuir* **2006**, *22*, 2299–2303.

(51) Würthner, F. *Chem. Commun.* **2004**, 1564–1579.

(52) Langhals, H. *Helv. Chim. Acta* **2005**, *88*, 1309–1343.

(53) Turro, N. J., *Modern Molecular Photochemistry*; University Science Books: 1991.

(54) Cui, H.; Hodgdon, T. K.; Kaler, E. W.; Abezgauz, L.; Danino, D.; Lubovsky, M.; Talmon, Y.; Pochan, D. *J. Soft Matter* **2007**, *3*, 945–955.

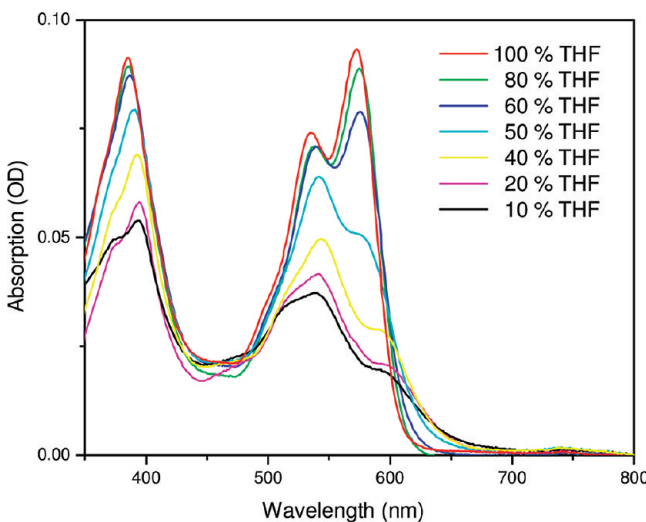


Figure 1. UV-vis spectrum of **PP2b** (2.4×10^{-6} M) in THF and different water/THF mixtures.

becomes inhomogeneous and **PP2b** precipitates. We will denote homogeneous solutions of **PP2b** in water/THF mixtures with a large water content (≥ 80 vol%) as “*aggregated solutions*”, whereas the term “*disaggregated solution*” is used to refer exclusively to solutions in organic solvents such as THF and chloroform. As discussed below, aggregated solutions become very viscous at concentrations above 10^{-3} M and gelation is observed above a critical gel concentration (cgc) of $\sim 6 \times 10^{-3}$ M. Therefore, when referring to **PP2b** at the cgc or above, the term “*supramolecular gel*” or just “*gel*” is used.

Cryogenic transmission electron microscopy (cryo-TEM) of water/THF solutions (80:20, v/v) of **PP2b** reveals the presence of uniform fibrous structures (Figure 2a,b). The width of the fibers is 3.3 ± 0.4 nm, while they reach remarkable lengths of $1\ \mu\text{m}$ or more. The fibers form ordered structures, as manifested by alternating dark high-contrast regions separated by regular spacings of 3.9 ± 0.4 nm. The darker-contrast regions represent tightly stacked conjugated systems that possess high electron density, while the lighter-contrast spacings represent a solvated shell of hydrophilic PEG tails.⁵⁴ The total width of a single fiber (inner aromatic core region and outer PEG shell) is 7.2 ± 0.8 nm. Upon increase in concentration, denser ordered structures are observed (Figure 2b). Individual fibers consist of segments of 2.0 ± 0.3 nm height (Figure 2b, arrow), representing a rare example of segmented supramolecular fibers,^{55,56} which we have also observed in several PDI-based self-assembled systems.^{41,57} The width of the nanofibers appears to be uniform over a wide range of concentrations (1.7×10^{-5} – 3.3×10^{-3} M). Figure 2c shows the possible structure of the supramolecular fibers, based on molecular modeling (see Supporting Information).

In addition to their remarkable aspect ratio and high degree of organization, the nanofiber assemblies appear to form large mechanically stable structures, as they can be filtered off from the water/THF solution (80:20, v/v) using standard PTFE syringe

filters with a $0.2\ \mu\text{m}$ pore size (Figure 3a). The filtrate is colorless, indicating essentially quantitative removal of the dye aggregates. Further evidence supporting the formation of extended structures in solution was gained from an experiment, in which a layer of water/THF mixture (80:20, v/v) was carefully added on top of a 10^{-4} M solution of **PP2b** in the same solvent, and the system was monitored to document mixing (Figure 3b–d). The photographs show the samples after 1 min (b), 6 h (c) and 4 days (d), indicating that almost no mixing is observed on the time scale of several days. Interestingly, such “nonmixing” behavior is typical of fully swelled gels, where addition of a solvent does not change the gel volume,⁵⁸ suggesting that **PP2b** forms a gel-like three-dimensional supramolecular network in aqueous solution.

Further insight into the solution-phase structure was obtained using cryogenic scanning electron microscopy (cryo-SEM, see Supporting Information for details), which is a methodology of choice for studying solvated three-dimensional networks.^{59,60} Cryo-SEM images reveal that in a fluid aggregated solution the nanofibers form an interconnected three-dimensional network (Figure 4). The majority of the fibers have widths of 6.5 ± 1.0 nm. Subtracting the thickness of the metal layer used for the imaging (~ 0.6 nm), the actual fiber width is 5.9 ± 1.0 nm, corresponding to the 7.2 ± 0.8 nm fiber width observed in cryo-TEM. The slightly smaller width observed in cryo-SEM can be due to a shrinkage of the PEG shell around the fibers caused by the sublimation of solvent from the vitrified gel during sample preparation (see Supporting Information).

Supramolecular Gel. In water/THF mixtures that contain between 10 and 20 vol% THF, **PP2b** forms gels above the critical gel concentration (cgc = 6×10^{-3} M), as evidenced by the rheological data (Figure 5) and vial inversion test (Figure 6a, inset). The gel was prepared by dissolving **PP2b** in THF in a vial, followed by the quick addition of water and vigorous shaking of the sample. Gelation takes place instantaneously. Rheological measurements reveal an elastic response; i.e., the storage modulus is larger than the loss modulus ($G' \gg G''$), and a pronounced plateau region of these moduli plotted against the frequency (Figure 5a), which is a characteristic feature of gels.⁶¹ The moduli are invariant over a wide range of strain (Figure 5b), revealing the gel response as a solid material even under large deformations.⁶¹

Once prepared, the gel is stable at room temperature in the presence of air and can be stored for several months without showing any change. The gel structure was studied by cryo-SEM, revealing an interconnected porous structure (Figure 6a) in which nanofibers create a three-dimensional network (Figure 6b). The smallest fibers have widths of 6.1 ± 1.1 nm, and their actual width (subtracting the thickness of the metal layer used for gel imaging (~ 0.6 nm)) is 5.5 ± 1.1 nm, similar to the size observed in the case of the solution-phase network. Furthermore, thicker fibers with various diameters have been observed, frequently branching out into smaller fibers. An additional distinctive characteristic is the presence of whirls and streams (Figure 6c,d). These anisotropic regions are several micrometers large and demonstrate a certain long-range order of the

- (55) Cui, H.; Chen, Z.; Zhong, S.; Wooley, K. L.; Pochan, D. J. *Science* **2007**, *317*, 647–650.
- (56) Li, Z.; Kesselman, E.; Talmon, Y.; Hillmyer, M. A.; Lodge, T. P. *Science* **2004**, *306*, 98–101.
- (57) Golubkov, G.; Weissman, H.; Shirman, E.; Wolf, S. G.; Pinkas I.; Rybtchinski, B. *Angew. Chem., Int. Ed.* **2009**, *48*, 926–930.

- (58) Yamauchi, A. Gels: Introduction. In *Gels Handbook*; Osada, Y., Kajiwara, K., Eds.; Academic: London, 2001; pp 4–12.
- (59) Matzelle, T.; Reichelt, R. *Acta Microscopica* **2008**, *17*, 45–61.
- (60) Menger, F. M.; Seredyuk, V. A.; Apkarian, R. P.; Wright, E. R. *J. Am. Chem. Soc.* **2002**, *124*, 12408–12409.
- (61) Kavanagh, G. M.; Ross-Murphy, S. B. *Prog. Polym. Sci.* **1998**, *23*, 533–562.

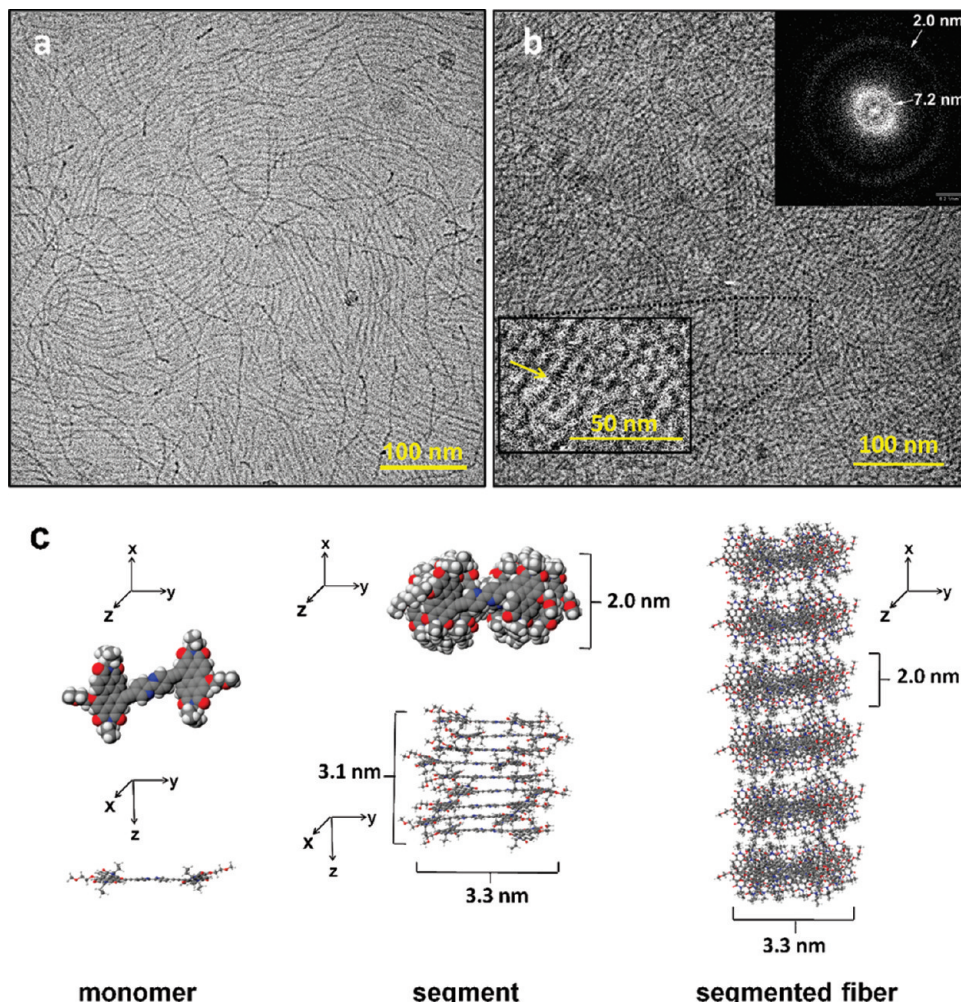


Figure 2. (a) Cryo-TEM image of **PP2b** aggregated solution (10^{-4} M) in water/THF mixture (80:20, v/v). The image shows ordered fibers (high contrast cores: 3.3 ± 0.4 nm, low contrast spacings: 3.9 ± 0.4 nm). (b) Cryo-TEM image of **PP2b** at higher concentration (3.3×10^{-3} M). Some individual fibers show distinct segments (yellow arrow). Inset: FFT calculation showing spacing of 7.2 nm (fiber–fiber distance) and 2.0 nm (segment–segment distance). (c) Molecular modeling of **PP2b** and its supramolecular structures. For simplification, PEG chains are modeled as the $-\text{O}(\text{CH}_2\text{--CH}_2)\text{OCH}_3$ group. Geometry optimization of the **PP2b** monomer was performed using the semiempirical PM3 method. The geometry of an individual segment and of the segmented fiber was optimized using the MM3 force field.

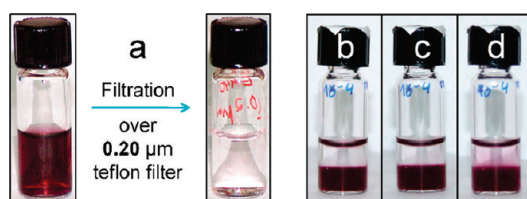


Figure 3. (a) Filtration experiment. The 10^{-4} M solution of **PP2b** was filtered over a PTFE syringe filter with $0.2 \mu\text{m}$ pore size. (b–d) Mixing experiment. A layer of water/THF mixture (80:20) was added on top of the aggregated solution of **PP2b** (10^{-4} M) in the same solvent mixture. The pictures are taken after (b) 1 min, (c) 6 h, and (d) 4 days.

supramolecular fibers within the gel. The structural anisotropies cause birefringence, as evidenced by polarized light microscopy (Figure 7). The observed morphologies and fiber widths are very similar in freshly prepared gel samples and in samples aged for a week, as observed in cryo-SEM images (Figure S5), consistent with rheological measurements that show a very similar elastic response in two samples.

UV-vis absorption spectra of the gel and aggregated solutions do not show a significant difference (Figure 8), confirming that the stacking geometry of the aromatic systems of **PP2b** is

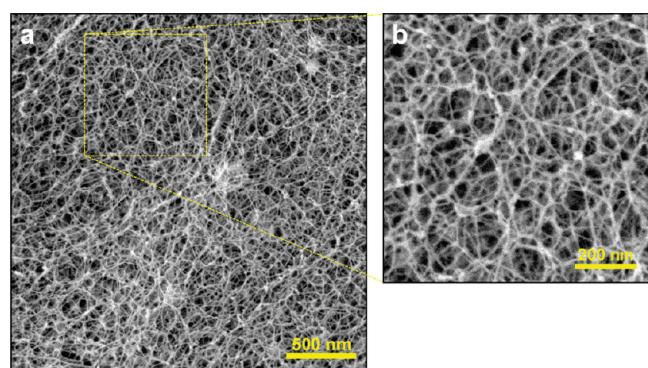


Figure 4. cryo-SEM images of an aggregated solution of **PP2b** (10^{-4} M) in water/THF mixture (80:20, v/v). (a) Extended network structure spanned by supramolecular fibers. (b) Magnified area. Individual fibers are 6.5 ± 1.0 nm in diameter.

identical in solution and in gel, as expected from the overall similarity of the solution-phase and gel morphology. The main difference between the gel and solution network structures is the density of the network and, in particular, the thickness of the fibers. Thus, while the solution-phase network is built mainly

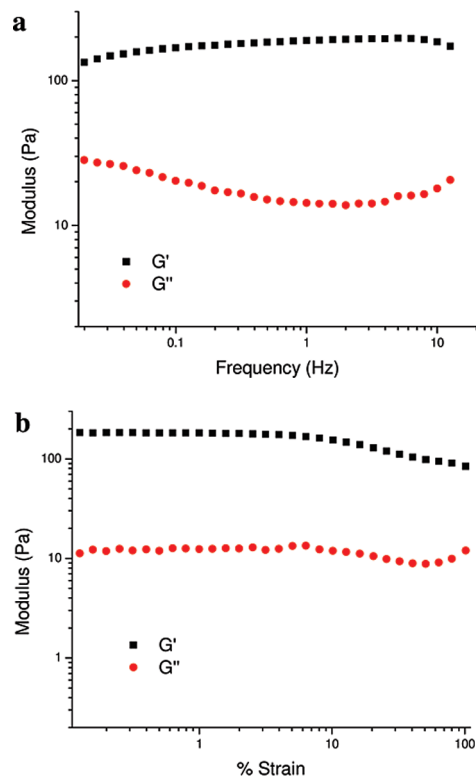


Figure 5. (a) Storage modulus, G' , and loss modulus, G'' , as functions of frequency, measured at 2% strain. (b) G' and G'' vs strain response measured at 1 Hz frequency.

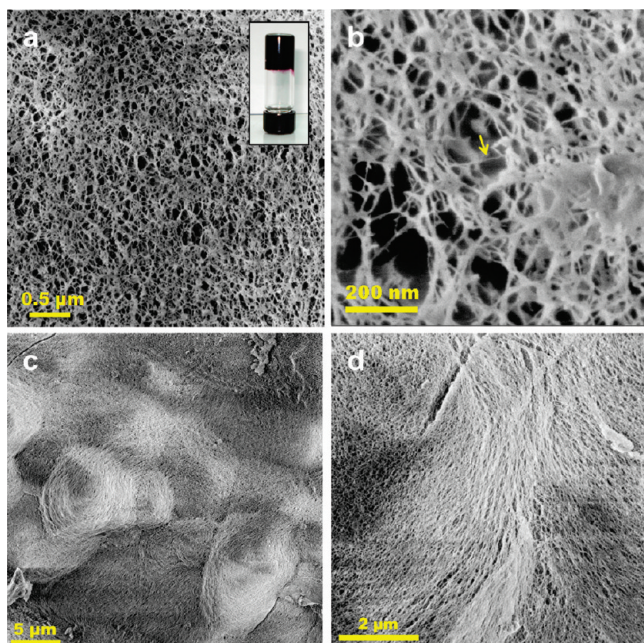


Figure 6. Cryo-SEM images of the gel of **PP2b** (8×10^{-3} M, water/THF mixture (80:20)) at different magnifications. (a) Nanoporous structure of the three-dimensional network. Inset: vial inversion test. (b) Image at high magnification shows three-dimensional network of nanofibers. The smallest fibers are 6.1 ± 1.1 nm in diameter (yellow arrow). (c) Whirs with diameters of $10\text{--}15$ μm . (d) Directional arrangement of fibers within a "microstream" in the gel.

from individual fibers and their thin bundles, the gel contains essentially thicker fiber bundles (Figures 4, 6), accounting for the greater mechanical strength of the gel.

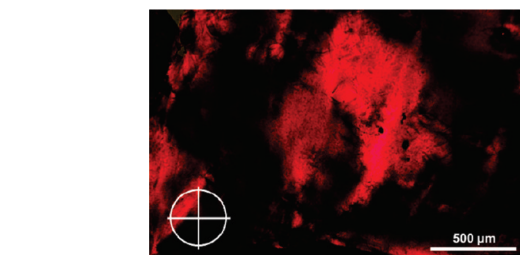


Figure 7. Polarized light microscopic image of the gel of **PP2b** (8×10^{-3} M) in water/THF mixture (80:20, v/v). The white cross indicates the orientations of the polarizing filters.

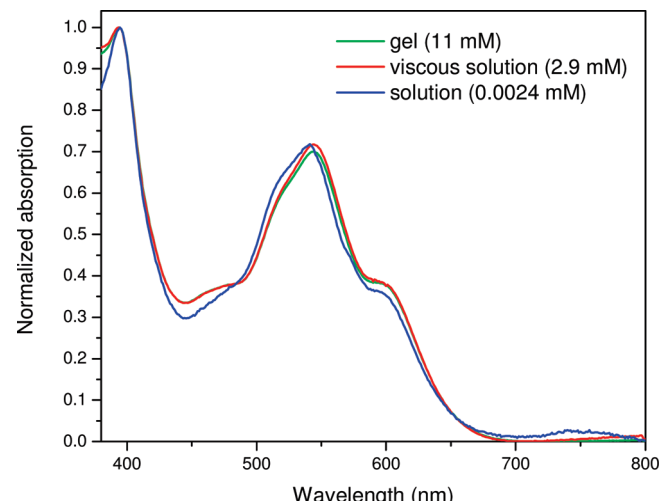


Figure 8. Normalized UV-vis absorption spectra of **PP2b** in water/THF mixture (80:20, v/v) at different concentrations, corresponding to gel (green trace), viscous solution (red trace), and dilute solution (blue trace).

We anticipate that the structure of the supramolecular fibers in both gel and solution follows the same hierarchy of self-assembly. The proposed assembly sequence, schematically depicted in Figure 9, is based on molecular modeling studies (Figure 2c) and electron microscopy data. On a first hierarchical level, the hydrophobic effect and $\pi-\pi$ interactions cause face-to-face stacking of **PP2b** into small aggregates of 8–10 molecules. Stacked molecules are shifted in respect to each other, due to the steric bulk of the ethylpropyl substituents attached to the imides in PDI. On a second hierarchical level, the hydrophobic effect is the driving force for further aggregation, this time driven by the aliphatic side chains of PDI imide substituents that, as a result of PDI stacking, form a substantial hydrophobic domain. Their interaction results in fibers with distinct segmentation. Then the fibers assemble into entangled bundles.⁴⁹ Branching out of these might provide a mechanism for the creation of junctions.⁶² Strong interactions between the fibers are most probably due to the significant residual hydrophobicity of the fiber interface.

Stimuli-Responsiveness. PDI systems are prone to reduction, some of them forming stable mono- and dianions in an aqueous medium^{63,64} that can be converted back to neutral PDI upon exposure to air.⁶³ We have recently shown that this aromatic charge/discharge cycle can be utilized for reversible depolymerization of supramolecular polymers.⁴¹

(62) Keller, A. *Faraday Discuss.* **1995**, *101*, 1–49.

(63) Shirman, E.; Ustinov, A.; Ben-Shitrit, N.; Weissman, H.; Iron, M. A.; Cohen, R.; Rybtchinski, B. *J. Phys. Chem. B* **2008**, *112*, 8855–8858.

(64) Marcon, R. O.; Brochsztajn, S. *J. Phys. Chem. A* **2009**, *113*, 1747–1752.

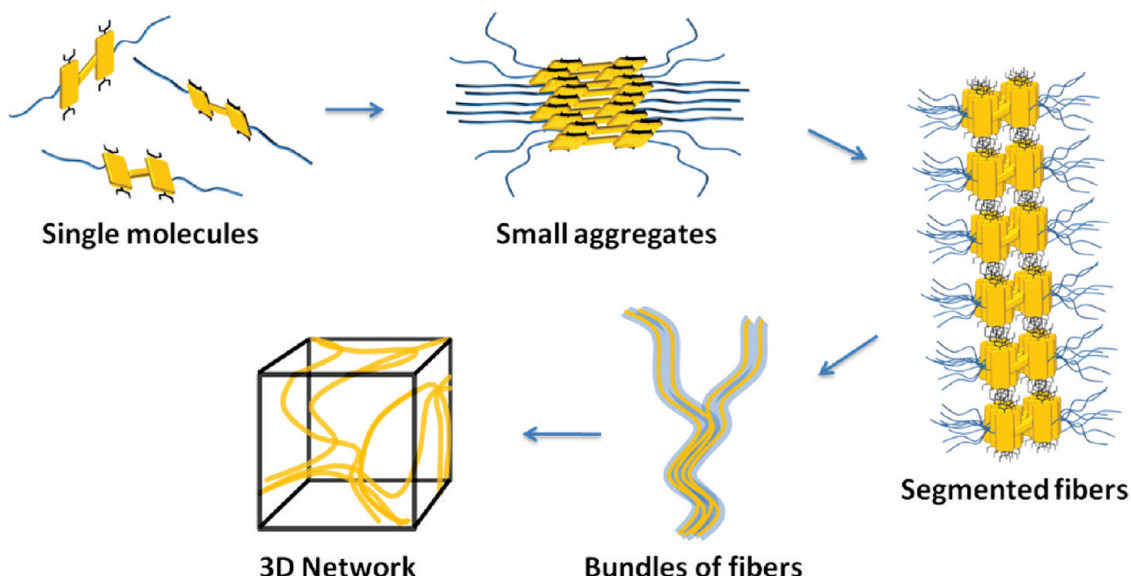


Figure 9. Schematic illustration of the PP2b assembly hierarchy.

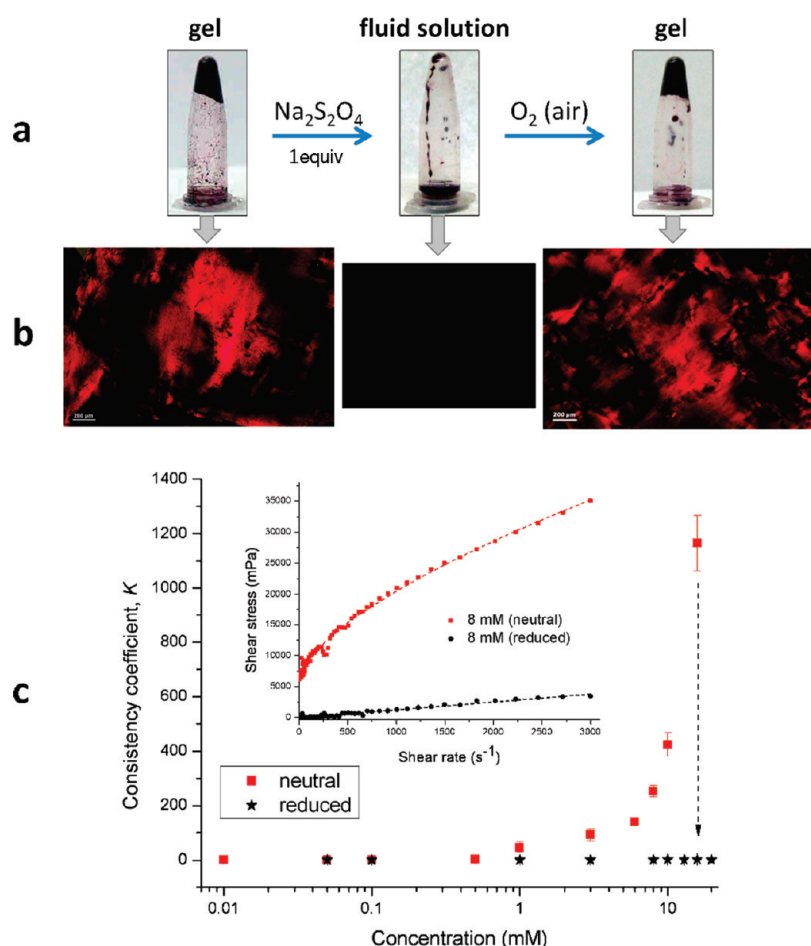


Figure 10. Effect of reversible charging of the gel in water/THF mixture (85:15, v/v). (a) Inverted tubes of the gel (8×10^{-3} M) before reduction, after reduction with 1 equiv of $Na_2S_2O_4$, and after oxidation back to the neutral state using air. (b) Polarized light microscopic images of the corresponding samples. (c) Plot of the consistency coefficient K as a function of the concentration of **PP2b** in water/THF mixture (85:15) for the neutral form (red) and the reduced form (black). The reduced samples are always fluid solutions. Inset: An example of a plot of shear rate vs shear stress for neutral sample and reduced sample (8×10^{-3} M).

Addition of an aqueous solution of 1 equiv of sodium dithionite to the supramolecular gel under an inert atmosphere causes a dramatic loss of viscosity, creating a fluid solution within several seconds (gel to sol transition, Figure 10). Ex-

posure of the resultant solution to air restores the gel within 10 min. The process is reversible and can be repeated at least three times. The transition of the gel to the fluid solution by reduction is accompanied by a loss of birefringence, which is restored

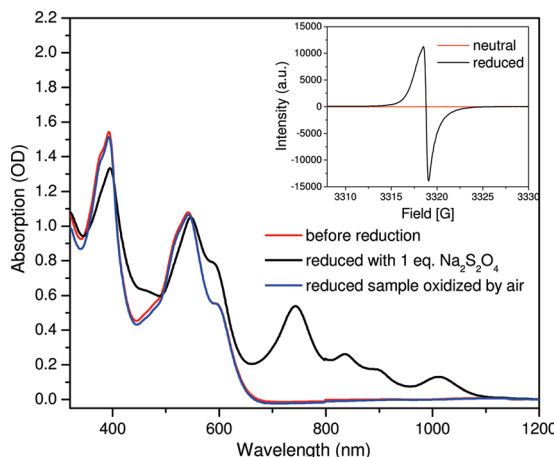


Figure 11. UV-vis spectra of aggregated solutions of **PP2b** (10^{-4} M) in water/THF mixture (80:20, v/v) before reduction (red), after reduction (black), and after exposing the reduced sample to air (blue). Inset: EPR spectrum of neutral (red) and reduced form (black).

after exposing the reduced fluid to air (Figure 10b). Thus, the structural change triggered by reversible charging causes the reversible switching of optical properties.

The reduced form shows a peak in the EPR spectrum, indicating paramagnetic species (Figure 11, inset), while the UV-vis spectrum of the reduced system shows four peaks in the near-infrared region, which represent a spectral signature of PDI radical anions (Figure 11).^{63–65} Formation of the radical anions leads to the destruction of the gel network, most probably due to electrostatic repulsion and better solvation of the more polar anion species resulting in fission of the nanofibers. The UV-vis spectrum recorded after exposing the reduced sample to air is identical to that of the unreduce form, showing that reduced species are oxidized back to their neutral state by atmospheric oxygen (Figure 11). No evidence of decomposition is found after the reduction/oxidation cycle, indicating that the charging/discharging sequence is fully reversible.

The influence of reducing agent on the viscosity of **PP2b** at concentrations between 10^{-5} M (dilute aggregated solution) and 2×10^{-2} M (gel) in water/THF (85:15, v/v) was investigated by rheological measurements (Figure 10c). Neutral samples exhibit shear thinning behavior (Figure 10c, inset), which is characteristic of linear polymers and wormlike aggregates that become aligned in the shear flow during the measurement.⁶⁶ In addition, samples with concentrations above the cgc show a yield stress, which is the finite stress required to achieve flow. The consistency coefficient K (measure of viscosity independent of shear rate) is obtained from fitting the shear rate vs shear stress plots to the standard Herschel–Bulkley model, $\sigma = K\dot{\gamma}^n + \sigma_0$, where σ is the shear stress, $\dot{\gamma}$ is the shear rate, σ_0 is the yield stress, and n is the flow behavior index.⁶⁷ In the presence of sodium dithionite, K drops drastically and the shear rate vs shear stress plot shows almost Newtonian behavior with no yield stress, even at high concentrations (Figures 10c (inset), S8). This dramatic drop in viscosity corroborates the destruction of the gel network. Oxidation results in restoration of the rheological behavior of the neutral systems, and the gel restores its initial elastic response (Figure S9).

(65) Gosztola, D.; Niemczyk, M. P.; Svec, W.; Lukas, A. S.; Wasielewski, M. R. *J. Phys. Chem. A* **2000**, *104*, 6545–6551.

(66) Dreiss, C. A. *Soft Matter* **2007**, *3*, 956–970.

(67) Steffe, J. F. *Rheological Methods in Food Process Engineering*; Freeman Press: 1996.

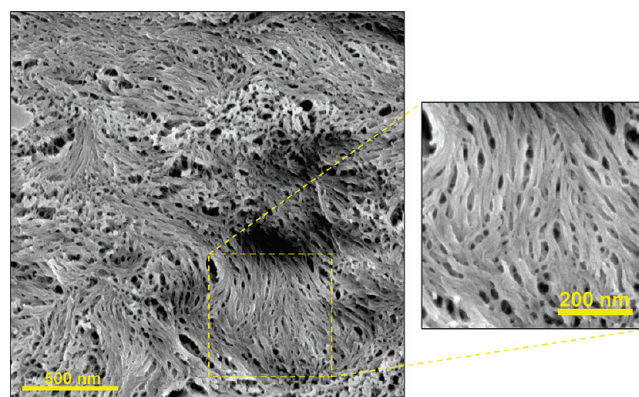


Figure 12. Cryo-SEM image of the thermally shrunken gel of **PP2b** (8×10^{-3} M, water/THF mixture (80:20)).

The supramolecular structure of the gel after a reduction/oxidation cycle is indistinguishable from that observed prior to this cycle, as evidenced from cryo-SEM images (compare Figures 6 and S6). The restoration of the supramolecular structure is essential for the reversibility observed in the switching of rheological properties and birefringence.

The gel also shows a remarkable temperature-dependent behavior. Commonly, supramolecular gels exhibit a thermally reversible gel/sol phase transition at moderate temperatures because of the weak noncovalent interactions involved in gelation.⁵ In contrast, the **PP2b** gel is stable toward change in temperature: it can be heated to 70 °C for at least 1 h without showing any change. Apparently, neither fiber fission occurs at this temperature nor the entanglement of the fibers is substantially weakened, which highlights the robustness of the noncovalent bonding responsible for the self-assembly of **PP2b**. Further heating to 100 °C does not lead to gel/sol phase transition. Instead, shrinkage of the gel is observed, leading to expulsion of a large fraction (~75 vol %) of the clear solvent mixture (Figures 13, S10). The shrinkage process is very rapid¹¹ (full shrinkage after only 90 s) and represents a rare example of the thermally triggered deswelling of a supramolecular gel.¹² Cryo-SEM of the shrunken gel reveals a very dense network of thick fiber bundles (Figure 12). Cavities between these bundles are much smaller than those in the swollen gel. The shrinkage is most probably due to a complex interplay between the hydrophobic effect and solvation of PEGs at higher temperatures.

The shrinkage is reversible in several ways. When slowly cooling the shrunken gel to room temperature, it expands spontaneously to its original volume. However, the swelling process is slow and completed only after ~24 h (Figure S10). The swollen gel form can be restored faster than that by sonication the sample for 1 h at ~40 °C.

The fastest way to restore the swollen gel is by exploiting the stimuli-responsiveness toward chemical reduction/oxidation. Addition of 1 equiv of aqueous sodium dithionite (at room temperature in the presence of air) to the solution surrounding the shrunken gel creates a temporarily fluid solution of reduced **PP2b**, followed by its gelation within several minutes due to oxidation by atmospheric oxygen (Figure 13). The temperature-triggered deswelling was repeated three times using sonication and another three times using reversible charging for restoration of the swollen gel, without any change in its responsiveness. Oscillatory rheological measurements show that the elastic response of the gel is fully restored after a shrinkage/swelling cycle (Figure S9). The switching between swollen gel, shrunken

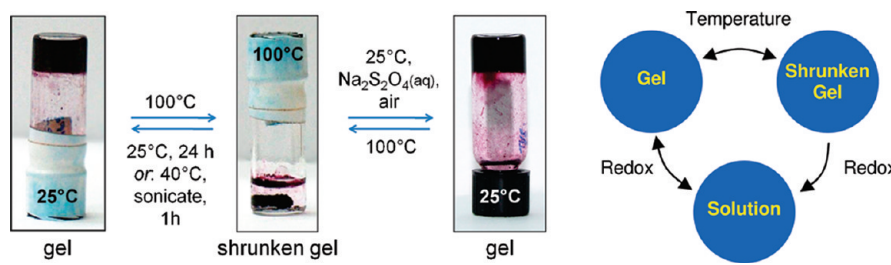


Figure 13. Left: Shrinkage of the gel of **PP2b** (8×10^{-3} M, water/THF (80:20, v/v)) in response to the rise in temperature. The completely swollen gel is obtained back after 24 h at room temperature. It can be obtained more rapidly by either sonicating at 40 °C for 1 h or by addition of 1 equiv of $\text{Na}_2\text{S}_2\text{O}_4$ (aq) in the presence of air. Right: Reversible switching between swollen gel, shrunken gel, and solution by exploiting response to temperature and reversible charging.

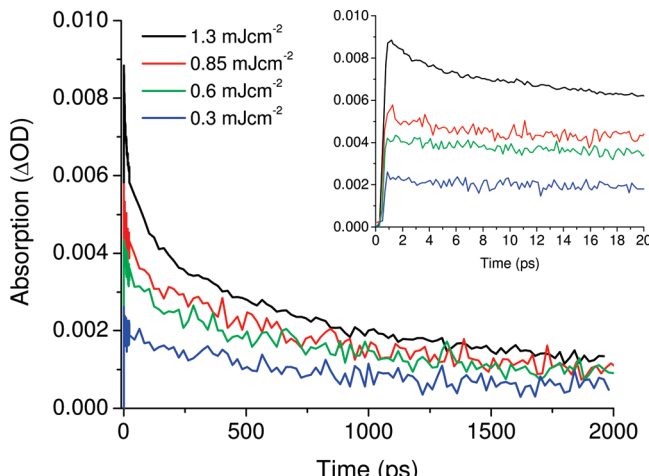


Figure 14. Decay kinetics of an aggregated **PP2b** (10^{-4} M) solution in water/THF (80:20, v/v) pumped at different energies and probed at the absorption peak (735 nm). The inset shows the first 20 ps of the transients.

gel, and fluid solution by exploiting dual responsiveness is depicted schematically in Figure 13. Such interconnected responsiveness allows great latitude in the design of functional adaptivity, which together with robustness may be useful for construction of self-assembled multiresponsive systems.

Energy Transfer. Relevant to light harvesting applications, **PP2b** assemblies strongly absorb visible light (Figure 8), while interactions between the chromophore units are expected to result in efficient excitation energy transfer. Femtosecond transient absorption studies on the disaggregated and aggregated **PP2b** (solution and gel state) reveal multiexponential decay of the excited state features. In the disaggregated state (chloroform solution, Figure S11, Table S1) the decays do not show power dependence, while the aggregated state (solution and gel) is characterized by power dependent kinetics (Figures 14, 15, S12, S13; Tables 1, 2). The power dependent decay in samples containing aggregated **PP2b** indicates that exciton annihilation takes place, which is typical of chromophore aggregates where a high photon flux of a laser pulse results in multiple excitations that bring about exciton annihilation processes. The complex power-dependent behavior may be attributed to various annihilation processes (delocalized and localized excitons, complex high-order multiexciton processes),⁶⁸ complicating the elucidation of energy transfer patterns.

Employing a widely used approximation, the site-to-site exciton hopping time constant, τ_{hop} , can be estimated from the

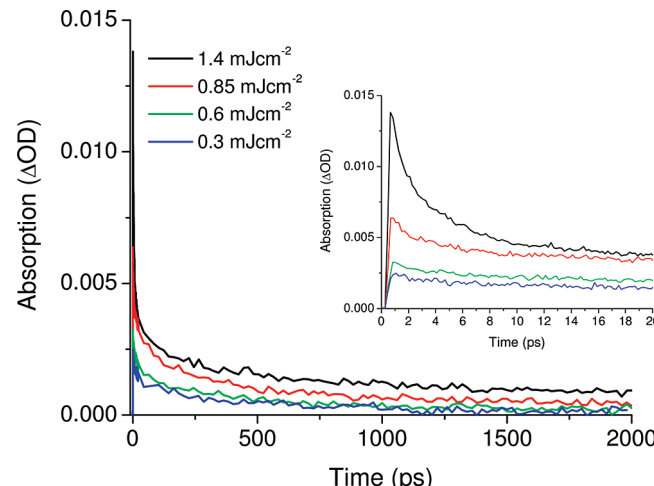


Figure 15. Decay kinetics of the gel sample of **PP2b** (8×10^{-3} M) in water/THF (80:20, v/v) pumped at different energies and probed at the absorption peak (725 nm). The inset shows the first 20 ps of the transients.

Table 1. Time Constants and Their Amplitudes (In Parentheses) Contributing to the Decay Kinetics of the Transient Absorption Spectrum (See Supporting Information) of an Aggregated Solution of **PP2b** (10^{-4} M) in Water/THF (80:20, v/v), Excited with Different Pump Fluences^a

pump fluence PP2b molecules per photon	1.3 mJ cm^{-2}	0.85 mJ cm^{-2}	0.6 mJ cm^{-2}	0.3 mJ cm^{-2}
	2.4	3.5	5.2	10.4
τ_1/ps	1.65 (0.20)	1.6 (0.18)	1.5 (0.12)	5.4 (0.12)
τ_1/ps	1.65 (0.20)	1.6 (0.18)	1.5 (0.12)	5.4 (0.12)
τ_2/ps	20 (0.23)	36 (0.17)	23 (0.13)	40 (0.10)
τ_3/ps	261 (0.26)	400 (0.28)	280 (0.27)	560 (0.34)
τ_4/ps	>2000 (0.31)	>2000 (0.36)	>2000 (0.48)	>2000 (0.43)

^a The number of **PP2b** per photon (based on laser power; see Supporting Information) is also given.

annihilation time constant, τ_{an} (corresponding to τ_1 and τ_2), using an “exciton random walk” model that has been shown to give satisfactory results for both natural and artificial chromophore aggregates.^{69,70} According to this model $\tau_{\text{an}} = (\pi^{-1}N \ln N + 0.2N - 0.12)\tau_{\text{hop}}$, where N is the number of hopping sites. Using the kinetics components for the two fastest processes (τ_1 and τ_2) and the calculated number of hopping sites, we could estimate the corresponding hopping times of ~ 300 fs and ~ 4 ps for the gel, along with ~ 800 fs and ~ 12 ps for the solution.

(69) Montroll, E. W. *J. Math. Phys.* **1969**, *10*, 753–765.

(70) Ahrens, M. J.; Sinks, L. E.; Rybtchinski, B.; Liu, W.; Jones, B. A.; Giaimo, J. M.; Gusev, A. V.; Goshe, A. J.; Tiede, D. M.; Wasielewski, M. R. *J. Am. Chem. Soc.* **2004**, *126*, 8284–8294.

Table 2. Time Constants and Their Amplitudes (in Parentheses) Contributing to the Decay Kinetics of the Transient Absorption Spectrum of the Gel of **PP2b** (8×10^{-3} M) in Water/THF (80:20, v/v), Excited with Different Pump Fluences (See Supporting Information)^a

pump fluence PP2b molecules per photon	1.4 mJ cm ⁻²	0.85 mJ cm ⁻²	0.6 mJ cm ⁻²	0.3 mJ cm ⁻²
	3.7	6.2	9.4	18.7
τ_1/ps	0.6 (0.45)	1.7 (0.38)	2 (0.27)	2.3 (0.29)
τ_2/ps	5 (0.31)	29 (0.23)	26 (0.23)	45 (0.23)
τ_3/ps	130 (0.15)	290 (0.25)	250 (0.32)	435 (0.32)
τ_4/ps	>2000 (0.09)	>2000 (0.14)	>2000 (0.18)	>2000 (0.16)

^a The number of **PP2b** per photon (based on laser power, see Supporting Information) is also given.

By using a similar model derived for a three-dimensional cubic lattice,⁶⁹ we obtained hopping times of \sim 150 fs and \sim 2 ps for the gel as well as \sim 300 fs and 4 ps for the solution. For comparison, the hopping time constants observed for various self-assembled PDI aggregates are similar (and analogous to the ones observed in natural light harvesting systems) to those we observe for **PP2b** assemblies: in aqueous solutions $\tau_{\text{hop}} = 220\text{--}900$ fs and 4–18 ps,⁵⁷ while in organic medium $\tau_{\text{hop}} = 5$ ps.⁷⁰ It should be noted that the estimation of hopping times is limited by the approximate character of the models. To distinguish between different possible modes of exciton delocalization in the complex hierarchical structures, development of models taking into account specific structural features of the systems will be needed.

Gels capable of excitation energy transfer have been suggested as promising systems for light harvesting.^{1,9,42,49,50,71} The good exciton mobility, excellent light absorption properties, and stability toward heat and light suggest that the gel based on **PP2b** represents an advantageous light harvesting scaffold. Whereas several *organogels* based on PDI derivatives have been developed and suggested for application as light harvesting structures, sensors, and photonic devices,^{46–48,72,73} the system presented herein is based on hydrophobic interactions, having

- (71) Ajayaghosh, A.; Praveen, V. K. *Acc. Chem. Res.* **2007**, *40*, 644–656.
- (72) Li, X.-Q.; Stepanenko, V.; Chen, Z.; Prins, P.; Siebbeles, L. D. A.; Würthner, F. *Chem. Commun.* **2006**, 3871–3873.
- (73) Seki, T.; Yagai, S.; Karatsu, T.; Kitamura, A. *Chem. Lett.* **2008**, *37*, 764–765.

many characteristics of *hydrogels*. To the best of our knowledge, PDI-based hydrogels have not been reported.

In conclusion, we have demonstrated that in aqueous media **PP2b** self-assembles into extended supramolecular fibers that form a robust three-dimensional network structure resulting in gelation. This supramolecular gel shows robustness and multiple stimuli-responsiveness. Reversible charging of **PP2b** allows for switching between the gel state and fluid solution. Simultaneously, this provides a method for switching on and off the material's birefringence. Temperature triggered shrinkage of the gel leads to the (reversible) expulsion of a large fraction of the aqueous solvent. The dual sensibility toward chemical reduction and temperature with distinct and interrelated response to each of these stimuli allows for adaptive behavior and convenient property switching. In addition to stimuli-responsiveness, excellent light absorption and exciton mobility characteristics of the gel render it valuable as a scaffold for light harvesting applications.

Acknowledgment. This work was supported by grants from the Israel Science Foundation (Grant No. 917/06) and the Helen and Martin Kimmel Center for Molecular Design. The cryo-EM studies were conducted at the Irving and Cherna Moskowitz Center for Nano and Bio-Nano Imaging (Weizmann Institute). Transient absorption studies were performed at the Dr. J. Trachtenberg laboratory for photobiology and photobiotechnology (Weizmann Institute) and were supported by a grant from Ms. S. Zuckerman (Toronto, Canada). B.R. holds the Abraham and Jennie Fialkow Career Development Chair. We thank Prof. Samuel Safran for valuable discussions; Dr. Lev Weiner for EPR measurements; Dr. Nir Kampf, Jehonatan Shachaf, and Ehud Yarom for assistance with rheological measurements; the group of Prof. Lia Addadi for access to the optical microscope; and the groups of Profs. Jacob Klein, Victor Steinberg, and Dror Seliktar for access to their rheometers.

Supporting Information Available: Experimental details of synthesis and characterization of **PP2b**, additional electron microscopy images. This material is available free of charge via the Internet at <http://pubs.acs.org>.

JA903938G